

# Seismically induced soft-sediment deformation structures in the Palaeogene deposits of the Liaodong Bay Depression in the Bohai Bay basin and their spatial stratigraphic distribution



Lei Liu <sup>a</sup>, Yijiang Zhong <sup>a</sup>, Hongde Chen <sup>a,b</sup>, Changgui Xu <sup>c</sup>, Kui Wu <sup>c</sup>

<sup>a</sup> Institute of Sedimentary Geology, Chengdu University of Technology, Chengdu 610059, China

<sup>b</sup> State Key Laboratory of Oil & Gas Reservoir Geology and Exploitation (Chengdu University of Technology), Chengdu 610059, China

<sup>c</sup> Tianjin Branch of CNOOC China Ltd., Tianjin 300452, China

## ARTICLE INFO

### Article history:

Received 1 May 2016

Received in revised form 17 June 2016

Accepted 19 June 2016

Available online 29 June 2016

Editor: Dr. B. Jones

### Keywords:

Deformation structures

Seismites

Spatial stratigraphic distribution

Cores

Liaodong Bay

## ABSTRACT

Soft-sediment deformation structures (SSDS) have been identified from well cores in the Palaeogene deposits of the Liaodong Bay Depression in the Bohai Bay basin, China. These deposits formed as interbedded sand and mud at a delta front or on the slope toe of the prodelta. According to criteria proposed by previous research, we established that these SSDS were induced by earthquakes and that they can be divided into two groups: ductile deformation structures (plastic intrusions, ball-and-pillow structures, flame structures, boudinage structures, irregular convolute stratifications, and synsedimentary faults and folds) and brittle deformation structures (sand dykes and autoclastic breccias). Based on their level of deformation, size, and complexity, the SSDS were divided into three Groups, from weak to strong, to reflect the intensity of palaeo-earthquakes. With consideration of the palaeo-sedimentary environment, we proposed a model to account for the production and preservation of these SSDS. According to the classification adopted in this study and the spatial stratigraphic distribution of the SSDS, the tectonic activities of the Tan–Lu faults in the Bohai Bay basin were investigated. The A and B oilfields (assumed names) are located in the tectonically active zones of the west and east branches of these faults, respectively. The extension tectonic activities in the A oilfield region exhibit a sharply decreasing trend from  $E_2s^3$  to  $E_2s^1$ , and increase again in  $E_3d^2$ ; whereas the strike-slip tectonic activities in the B oilfield region exhibit an increasing trend from  $E_2s^3$  to  $E_2s^1$ , and finally, reach a maximum to  $E_3d^3$ . The results of this study show that the method of analysis of the spatial stratigraphic distribution of SSDS is suitable for determining the evolution of tectonic activity and thus, it can provide a new perspective for basin analysis.

© 2016 Elsevier B.V. All rights reserved.

## 1. Introduction

Soft-sediment deformation structures (SSDS) and well cores can provide information of depositional history and reveal aspects of basin evolution. These deformation structures can form when sediments are unconsolidated or shortly after consolidation via many processes, e.g., earthquakes, rapid deposition in slumping environments, and storm waves (Owen, 1987, 1996; Allen, 1982). Whatever the trigger mechanism, the cause of SSDS can be attributed to a decrease of shear resistance and a collapse of the grain framework (Chaney and Fang, 1991). The types and scales of SSDS depend on the intensity of the trigger mechanism, physical properties of the sediments, and sedimentary environment (Berra and Felletti, 2011). SSDS have been observed and studied in many areas in various sedimentary environments, especially

lacustrine (Scott and Price, 1988; Rodríguez-Pascua et al., 2000; Galli, 2000). Because of the diversity of trigger mechanisms, it is especially important to judge their origin by the distinguishing criteria. The criteria, proposed and elucidated by Sims (1975), Owen and Moretti (2011), used to identify palaeo-earthquakes are as follows. (1) SSDS are deformed in a tectonically active basin near an active fault. (2) SSDS recur in the vertical direction, separated by undeformed beds, and develop continuously in the lateral direction. (3) The morphologies of SSDS are comparable with deformation structures confirmed from active earthquake belts. (4) SSDS occur in complex combinations. (5) Both deformed and undeformed beds develop in similar lithologies and facies (Montenat et al., 2007; Owen et al., 2011). It is necessary to exclude all other possible trigger mechanisms before SSDS can be identified as induced by earthquake. The indicator for storm-induced SSDS is the presence of typical storm deposits (hummocky cross bedding), which mainly develop in a marine basin. It is almost impossible that storm deposits could be observed in a palaeo-lake

E-mail address: [172058088@qq.com](mailto:172058088@qq.com) (L. Liu).

environment because of the shallowness and the spatial dimension (Taşgın, 2011). The presence of coarse sediments can be indicative of rapid deposition in a slumping environment. Coarse sediments mainly develop with processes of mass transport, e.g., slumping, sandy debris, and turbidites or with over-steepening of depositional slopes (Owen and Moretti, 2011; Oliveira et al., 2011; Van Loon and Pisarska-Jamroz, 2014). Rapid sedimentation can only be preserved well where the overlying sediments are thick, massive and without grain size variation (Ghosh et al., 2010). The SSDS induced by earthquakes are seismites, which is a term proposed by Seilacher (1969) to describe layers that record palaeo-earthquake events. The theory of seismogenesis has been quoted frequently as the most appropriate for the interpretation of numerous SSDS (Alfaro et al., 2002; Jewell and Etensohn, 2004; Bachmann and Aref, 2005; Zhang et al., 2007; Ghosh et al., 2010; Berra and Felletti, 2011; Kundu et al., 2011; Martín-Chivelet et al., 2011; Moretti and Ronchi, 2011; Van Loon and Pisarska-Jamroz, 2014).

Various SSDS that present both as ductile and brittle deformation structures have been identified from well cores in the Palaeogene deposits of the Liaodong Bay Depression in the Bohai Bay basin (China). The characteristics of these SSDS accord with the criteria above; however, the possibility of the presence of storm or gravity deposits is discounted because of the absence of evidential indicators in study area. The absence of any evidence of hummocky cross bedding in the area excludes storm activities, and rapid deposition can be excluded because of the absence of coarse sediments, gravity flows, and the over-steepening of depositional slopes. Based on the criteria proposed by Montenat et al. (2007) and by Owen et al. (2011), it can be confirmed that the SSDS in the study area were induced by palaeo-earthquakes. In addition, analysis of their morphologies is useful in determining the mechanism of their formation. Many studies on seismites and palaeo-earthquakes have been conducted in other regions of the Bohai Bay basin, which have focused on the characteristic features of the seismites and on their development sequence (Chen et al., 2003; Yuan, 2004; Lu, 2004; Shi et al., 2009;). However, few studies have considered the characteristics of the SSDS in the Liaodong Bay Depression or discussed their trigger mechanism (Wang et al., 2008). A seimite sequence can reveal the process of an earthquake; however, it does not have the general applicability of the Bouma Sequence. This is because SSDS in different regions could have different sequences. Depending on the degree of consolidation of the deposits, seismic shock can cause different types of deformation structure, ranging from ductile to brittle. Therefore, based on the degree of liquefaction and deformation, the magnitudes and epicentres of palaeo-earthquakes can be deduced (Rodríguez-Pascua et al., 2010; Berra and Felletti, 2011; Pöldsaaar and Ainsaar, 2015).

The main objectives of this work are to identify typical deformation structures of the Palaeogene deposits of the Liaodong Bay Depression, analyse their sedimentary environments, and summarise their spatial stratigraphic distribution to deduce the palaeo-earthquake activity of the study area. These data and methods could be beneficial in further analyses of the tectonic evolution of the Liaodong Bay Depression and the characteristics of the tectonic activity of the basin-controlling Tan–Lu faults.

## 2. Study area

### 2.1. Geological setting

The Liaodong Bay Depression, which is a secondary tectonic unit of the Bohai Bay basin, is located in the northeast of the Bohai Bay basin in China. The Bohai Bay basin is a typical rifted basin on the North China Craton that is controlled by the Tan–Lu faults (Fig. 1a). The Liaodong Bay Depression is a deep and narrow rifted basin that has developed in alignment with the NE-trending Tan–Lu faults.

Multi-stage extensional and strike–slip fault activities have led to the special tectonic characteristics of the Liaodong Bay Depression, which

consist of three uplifts and two sags. From west to east, these are arranged as the Liaoxi Sag, Liaoxi Uplift, Liaozhong Sag, Liaodong Uplift and Liaodong Sag. The Tan–Lu faults developed across the Liaoxi and Liaozhong sags in a NE direction, bifurcating into two branched faults in the Palaeogene (Fig. 1b). These branched faults are dextral slip faults that have been studied by other researchers (Xu et al., 2005; Gong et al., 2007). The western faults predominantly exhibit extensional activity, whereas the eastern faults predominantly exhibit strike–slip activity. The Liaozhong Sag has the largest sedimentary thickness of the three sags, followed by the Liaoxi and Liaodong sags. Each tectonic unit has developed in the NE direction and they are aligned parallel to each other. The tectonic evolution of the Liaodong Bay Depression in the Palaeogene was related closely to the tectonic setting of the Bohai Bay basin, and controlled by the dextral strike–slip activity of the Tan–Lu faults. The tectonic evolution can be divided into three stages: extension and rifting in the Palaeocene to middle Eocene (56–38 Ma), post-rift thermal subsidence in the late Eocene to early Oligocene (38–32.8 Ma), and strike–slip and rifting activity in the Dongying period of the Oligocene (32.8–24.6 Ma) (Zhu et al., 2008; Zhao et al., 1996) (Fig. 2).

### 2.2. Material and methods

The depositional characteristics of SSDS and their spatial stratigraphic distribution in the Palaeogene deposits of the Liaodong Bay Depression can be analysed based on observations and statistics of the core intervals in this area. These core intervals were obtained by the Tianjin Branch of CNOOC China Ltd. There have been 213 exploration and development wells drilled in the Liaodong Bay Depression and we used cores from 102 wells, whose intervals included Palaeogene deposits. However, of these, only 92 cores were available because some cores were destroyed or sealed by natural or human factors. Granulometry, sedimentary facies and structures were recorded in detail together with the description of SSDS. In the majority of available cores, there was no core loss. The lengths of the core intervals in the cored wells ranged from 0.86 to 143.38 m, with diameters of either 80 mm (slabbed) or 100 mm (not slabbed). Cores were split lengthwise, photographed with digital camera. Overall, over 80% of wells had core intervals of <40 m. The wells were distributed mainly in the Liaoxi Uplift, Liaozhong Sag, and Liaodong Uplift, and concentrated in the horizons of  $E_2s^3$ ,  $E_2s^2$ ,  $E_2s^1$ ,  $E_3d^3$ , and  $E_3d^2$  of the Palaeogene. SSDS were observed in 33 core intervals from 25 wells. Among these, 5 core intervals were located in  $E_2s^3$ ; 7 core intervals were located in  $E_2s^2$ ; 5 core intervals were located in  $E_2s^1$ ; 4 core intervals were located in  $E_3d^3$ ; and 12 core intervals were located in  $E_3d^2$ . The depths, horizons, sedimentary environments, and specific deformation structures of these core intervals with developed SSDS are shown in Table 1 to explain the depositional environments, trigger mechanisms, and distribution horizons of the SSDS. All the data gave significant information to analyse sedimentary characteristics of SSDS and helped deduce tectonic activities in spatial and stratigraphic aspects.

### 2.3. Sedimentological setting

The Palaeogene strata that (from old to new) consist of the Kongdian, Shahejie, and Dongying formations form the object of this research. The SSDS are concentrated mainly in the Shahejie and Dongying formations. The strata of the Shahejie Fm. can be divided into  $E_2s^4$ ,  $E_2s^3$ ,  $E_2s^2$ , and  $E_2s^1$  and the strata of the Dongying Fm. can be divided into  $E_3d^3$ ,  $E_3d^2$ , and  $E_3d^1$  (Fig. 2).

The sedimentary deposits of  $E_{1-2}$  k to  $E_2s^4$  are small-sized lacustrine facies and alluvial fan facies, the main lithologies of which are mudstone and carbonatite, formed in the early chasmic stage of the basin under a dry climatic background (Zhu et al., 2008). The shale or mudstone lithologies of  $E_2s^3$  are lacustrine facies that formed in the centre of the lake basin. In addition, fan-delta and near-bank submerged alluvial fan deposits are developed on the edge of the lake basin (Dong et al.,

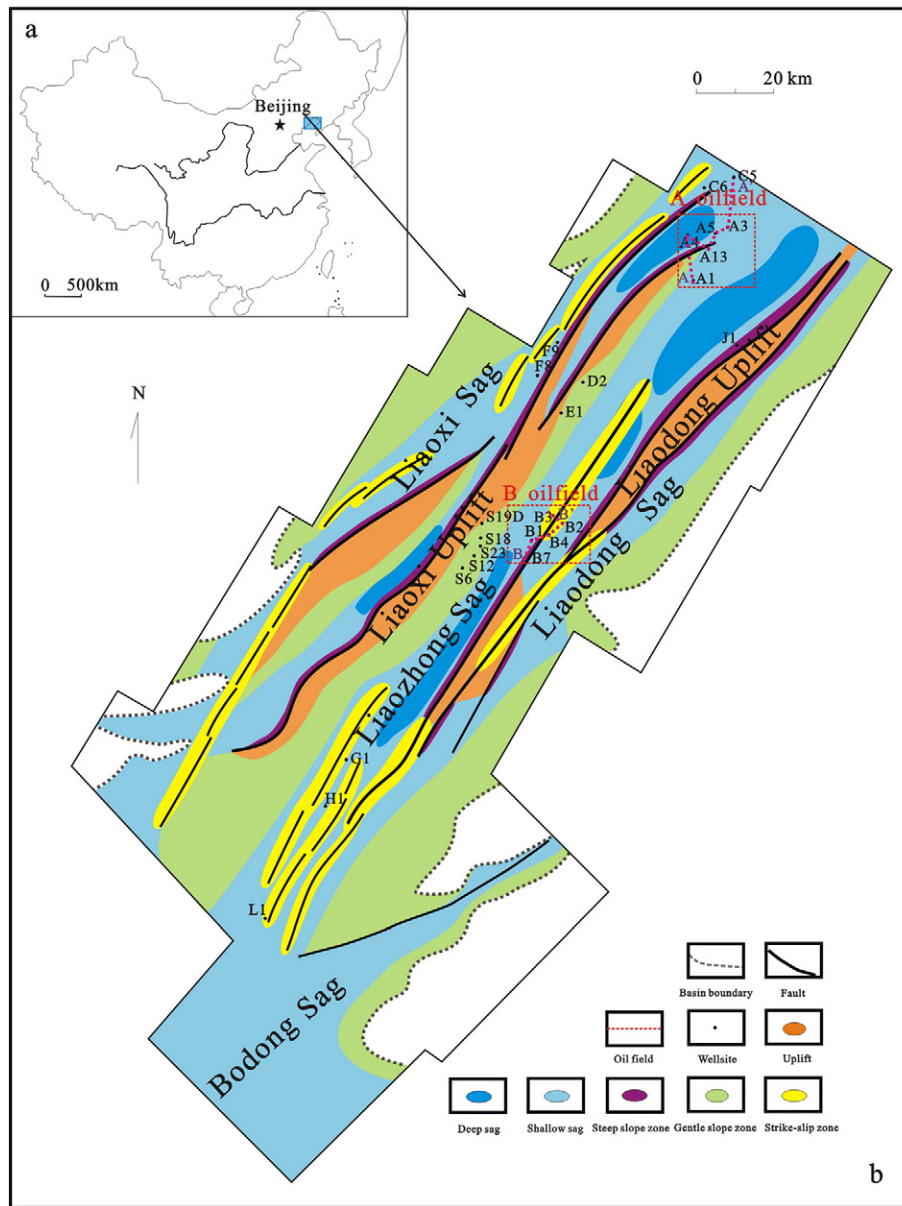


**Fig. 1.** Location and geological framework of the study region. (a) Location of the Liaodong Bay Depression in the Bohai Bay basin, China. (b) Geological setting of the Liaodong Bay Depression in the Palaeogene deposits, with the locations of A and B oilfields. Locations of A–A' and B–B'.

2007; Li et al., 2007). The  $E_2s^2$  stratum contains lacustrine facies and carbonate platform and fan-delta deposits, the main lithologies of which are interbedded grey mudstone or shale and medium-coarse sandstone. The  $E_2s^1$  stratum contains lacustrine facies and carbonate platform deposits, the main lithologies of which are dark mudstone, shale, and bioclastic limestone or dolostone (Dong et al., 2007; Zhu et al., 2008; Chang et al., 2014). This special lithologic section in the Bohai Bay basin can be used for regional comparison.

The Dongying Fm. has considerable thickness, which approximately ranges from 500 to 3000 m, reflecting the sedimentary environment transition from lacustrine facies to deltaic and fluvial facies. The sedimentary deposits of  $E_3d^3$  are mainly lacustrine facies of dark grey mudstone intercalated with sandstone lenses (Wang et al., 2008; Zhu et al., 2008). The stratum of  $E_3d^2$  contains mainly deltaic deposits of thick medium-fine sandstone or sub-lacustrine fan deposits with coarse-grained clastics that formed in a deep lake environment (Zhu et al., 2008; Wu et al., 2011). The deposits of  $E_3d^1$  are mainly fluvial, deltaic, and lacustrine facies whose lithologies are interbedded

yellow-grey mudstone and pale grey sandstone. Most of the  $E_3d^1$  stratum is missing in the research area because of tectonic uplift (Zhao et al., 1996; Xu et al., 2005; Zhu et al., 2008; Wu et al., 2011) (Fig. 2).

### 3. Description of the SSDS

Many types of SSDS may be observed in the lacustrine and deltaic facies of the Palaeogene layers of the Liaodong Bay Depression. The geometries and morphologies of the SSDS, which depend on the sedimentary environment and lithologies, have obvious distinctions between different areas. The deformation structures are developed mainly in the delta front, the lithologies of which comprise interbedded fine-medium sandstone and mudstone. The structures include plastic intrusions, ball-and-pillow structures, flame structures, boudinage structures, synsedimentary faults and folds, irregular convolute stratification, sand dykes, and autoclastic breccias. As proposed by Montenat et al. (2007) and Berra and Felletti (2011), we divided the observed SSDS into two main groups: ductile deformation structures and brittle structures.

Stage	Formation		Sub-member	Age(Ma)	Basin tectonic evolution stages	Sedimentary facies				
	No.	Member								
Oligocene	Dongying	No.1	E <sub>3</sub> d <sup>1</sup>	24.0	Strike-slip and rifting stage	Fluvial Delta				
		No.2	E <sub>3</sub> d <sup>2</sup>				Delta Shore-shallow lacustrine			
		Lower	Upper					Delta Sub-lacustrine fan		
							No.3		E <sub>3</sub> d <sup>3</sup>	Delta Sub-lacustrine fan Semi-deep and deep lacustrine
	Shahejie	No.1	E <sub>3</sub> s <sup>1</sup>	32.8		Post-rift thermal subsidence stage	Extinct rifting stage	Shore-shallow lacustrine Carbonate platform		
		No.2	E <sub>3</sub> s <sup>2</sup>					Fan-delta Delta Shore-shallow lacustrine		
		Lower	Middle			Upper	38.0	Extension and rifting stage	Intense rifting stage	Fan-delta Delta
										Shore-shallow lacustrine Semi-deep and deep lacustrine
No.4	E <sub>3</sub> s <sup>4</sup>	42.0	Initial rifting stage	Fan-delta Near-bank submerged alluvial fan						
No.3	E <sub>3</sub> s <sup>3</sup>			Fan-delta Shore-shallow lacustrine						
Paleocene	Kongdian			50.4	Initial rifting stage	Playa Alluvial fan				
				65.0						

Fig. 2. Stratigraphic framework and sedimentological setting of the Liaodong Bay Depression (modified from Zhu et al., 2008 and references therein).

3.1. Ductile deformation structures

3.1.1. Plastic intrusions

Plastic intrusions are mainly developed in interbedded sand and mud sediments. The fine material of such sediments intrudes vertically into the surrounding rocks and deforms the surrounding layers (Obermeier, 1996; Berra and Felletti, 2011). They are like diapir structures but they do not reach the surface. Either sand or mud sediment can act as intruded material when in liquefied condition (Fig. 3a, b). Generally, the breadth of the intruded sediment becomes narrower and it finally pinches out in the direction of intrusion. Irregular morphologies of such intrusions show that liquefied sediments are unidirectional. Similar deformation structures can be found in the surrounding sediments and at the boundary between the intruded sediment and surrounding rock (Fig. 3a, b).

Plastic intrusions are common structures in the study area. Based on well cores, it has been established that the breadths of the plastic intrusions range from 0.01–0.03 m and that their heights range from 0.03 to 0.10 m (Fig. 3a, b). Their scale depends on the consistency and grain size of the surrounding layers.

3.1.2. Ball-and-pillow structures

Ball-and-pillow structures are one of the most numerous deformation structures in the study area. These are characterised by a periodically arranged suite of pillows or balls composed of fine-grained sandstone. They are developed widely in interbedded layers of sand and mud. When overlying sandy sediments fall into underlying muddy layers, ball-and-pillow structures are formed, and both the overlying and the underlying layers exhibit liquefaction phenomena (Fig. 3i).

Liquefied sediments may remain connected with the parent rock, forming pillows. Such pillows, formed by liquefied sandstone, tend to be elliptical in shape when arranged laterally; however, they can also be arranged vertically, in which case they are upswept (Fig. 3e, f). The breadths of the individual pillows range from 2 to 5 cm, although they can remain interconnected each other. Portions of dense overlying liquefied sediments can become completely separated from the parent rock and form balls floating in the underlying less-dense sediment (Fig. 3c). Most of these balls are rounded or sub-rounded and isolated in the underlying sediment. The breadths of these balls range from 0.5–1.5 cm with horizontal spacing ranging from 1 to 5 cm. Small parts of the balls could form irregular shapes with distinct internal stratifications reflecting dragging and stretching morphologies (Fig. 3d).

3.1.3. Boudinage structures

Boudinage structures of differing sizes and complexities resemble the “looping–bedding” structures in lacustrine deposits of Miocene seismites described by Calvo et al. (1998). Boudinage structures are developed in interbedded sand and mud layers. Thin sandstone layers are sandwiched between mudstone layers in this lithology. Liquefied sandstone, which can become mixed with the mudstone, develops tensile deformation structures. Some of the deformed sediment forms lenticles, whereas some is pulled apart like boudinage. Some lenticles can become separated and arranged at intervals within the horizon (Fig. 3g). The isolated boudinage structures do not extend as far as their original sedimentary layers. The sizes of the deformations depend on the trigger mechanism and they are usually decametre-scale in breadth, centimetre-scale in height, and arranged at centimetre-scale intervals. These structures develop with other deformation structures such as flame structures and ball-and-pillow structures (Fig. 3g, h).

3.1.4. Flame structures

These structures are commonly developed in thin sandstone and mudstone interbedded layers. These flame structures tend to develop together with ball-and-pillow or boudinage structures (Fig. 3i). The morphologies of the flame structures tend to be symmetrical under liquefied conditions. Overlying liquefied sandy sediments can mix slightly with underlying mud sediments, such that liquefied mud sediments can be observed along the sandy layer. The breadths of the flame structures, which are clearly observed in well B1, are about 2–3 cm (Fig. 3i). In well A1, the flame structures are developed well in the underlying dark red pelitic strip with obvious liquefaction of the overlying sandstone (Fig. 3j).

3.1.5. Irregular convolute stratifications

Irregular convolute stratifications are structures induced by the liquefaction of sediments. They are characteristically inconsistent within a layer in respect of size, scale, and morphology and they exhibit highly distorted stratification. The thicknesses of such structures vary considerably from the decametre to metre scale. Although irregular convolute stratifications and synsedimentary folds have similar morphologies, the degree of liquefaction represented by the two types of structure is distinctly different. Irregular convolute stratifications, observed with other liquefied deformation structures, are generally present in fine-medium-grained sandstone (Fig. 4a), although they are sometimes mixed with coarse deposits. The original bedding of liquefied coarse sandy sediments is rarely preserved; however, the original bedding of the fine-grained sediments is usually conserved comparatively intact

**Table 1**  
SSDS statistics based on core intervals.

Well	Depth/m	Horizon	Deformation structures	Sedimentary environment
A1	2942.5–2938.8	E <sub>3</sub> d <sup>2</sup>	① ③ ⑤ ⑦ ⑧	Prodelta
	2634.9–2629.5	E <sub>3</sub> d <sup>2</sup>	① ② ④ ⑤ ⑥	Delta front
A13	3387.1–3382.8	E <sub>2</sub> s <sup>3</sup>	③ ⑦ ⑧	Prodelta
	2885.1–2879.3	E <sub>2</sub> s <sup>1</sup>	① ②	Shallow lacustrine
A4	3308.9–3306.1	E <sub>2</sub> s <sup>2</sup>	① ② ③	Delta front
A5	3217.6–3215.8	E <sub>2</sub> s <sup>2</sup>	① ③	Delta front
A3	3145.8–3141.8	E <sub>2</sub> s <sup>2</sup>	① ③ ⑤	Delta front
B7	1463.3–1462.2	E <sub>3</sub> d <sup>3</sup>	① ②	Delta front
B1	3036.4–3035.2	E <sub>2</sub> s <sup>2</sup>	①	Delta front
	2923.8–2919.2	E <sub>2</sub> s <sup>1</sup>	① ② ③ ④ ⑤	Delta front
	2756.2–2738.1	E <sub>3</sub> d <sup>3</sup>	① ② ③ ④ ⑤ ⑦	Delta front, Prodelta
B4	1760.2–1756.4	E <sub>2</sub> s <sup>1</sup>	② ③ ⑤ ⑥	Delta front
B2	1920.7–1918.6	E <sub>2</sub> s <sup>1</sup>	⑤ ⑥	Delta front
	1835.2–1837.5	E <sub>3</sub> d <sup>3</sup>	⑥ ⑦ ⑧	Delta front, Prodelta
	1147.8–1146.7	E <sub>3</sub> d <sup>2</sup>	③ ⑤ ⑥	Delta front
B3	3008.2–3003.6	E <sub>2</sub> s <sup>3</sup>	① ⑥	Delta front
C5	1698.4–1690.2	E <sub>3</sub> d <sup>2</sup>	② ③ ④ ⑤ ⑥	Delta front
C6	2549.9–2544.8	E <sub>2</sub> s <sup>2</sup>	② ⑤ ⑥	Delta front
D2	2587.7–2582.2	E <sub>2</sub> s <sup>2</sup>	① ③ ④ ⑤	Delta front
E1	2266.7–2265.1	E <sub>3</sub> d <sup>2</sup>	① ③	Delta front
J1	2826.6–2825.8	E <sub>3</sub> d <sup>3</sup>	①	Delta front
F8	2523.1–2521.9	E <sub>2</sub> s <sup>3</sup>	② ③ ④ ⑤ ⑥	Shallow lacustrine
F9	2014.5–2013.7	E <sub>2</sub> s <sup>2</sup>	① ②	Delta front
G1	3099.1–3096.2	E <sub>2</sub> s <sup>3</sup>	①	Shallow lacustrine
	2623.9–2622.6	E <sub>3</sub> d <sup>3</sup>	⑦ ⑧	Prodelta
H1	3005.3–3003.4	E <sub>2</sub> s <sup>3</sup>	③ ④ ⑤	Delta front
S6	1483.5–1482.5	E <sub>3</sub> d <sup>2</sup>	① ②	Delta front
S12	1405.8–1403.5	E <sub>3</sub> d <sup>2</sup>	② ⑥	Delta front
S18	1390.5–1383.3	E <sub>3</sub> d <sup>2</sup>	② ⑤	Delta front
S19D	1959.6–1952.5	E <sub>3</sub> d <sup>2</sup>	② ③ ⑤ ⑦	Delta front, Prodelta
S23	1546.3–1545.4	E <sub>3</sub> d <sup>2</sup>	② ③ ⑤ ⑦	Delta front, Prodelta
L1	2637.7–2631.8	E <sub>3</sub> d <sup>2</sup>	② ③ ④ ⑤ ⑥	Delta front
	2701.2–2705.5	E <sub>3</sub> d <sup>2</sup>	② ③ ⑤	Delta front

- ① Synsedimentary faults and folds   ② Plastic intrusions   ③ Ball-and-pillow structures   ④ Flame structures  
 ⑤ Boudinage structures   ⑥ Irregular convolute stratifications   ⑦ Sand dykes   ⑧ Autoclastic breccias.

(Fig. 4b). Generally, deformation structures in adjacent layers are eroded. Pure sandstone, present in the adjacent layers, forms abrupt contact with the SSDS.

### 3.1.6. Synsedimentary folds and faults

Synsedimentary faults and folds frequently occur in pairs, which indicates that the folds and faults have an inevitable contact and transformation between them (Fig. 4c). They are commonly observed along a layer and confined between undeformed layers, indicating that the process of this deformation occurs in unconsolidated or partly consolidated sediments (Rossetti and Góes, 2000). Synsedimentary faults, which are

usually tensional normal faults like stair-step faults, are mainly developed in parallel in thin sand–mud interbedded layers (Fig. 4e, f). These faults occur in either single or multiple groups. They appear as centimetre-scale discontinuities in stair-step or listric style, which are typically confined between two undeformed layers. On occasion, they can be seen with a “normal flower structure” (Fig. 4d), such as in a strike–slip fault. The offset of these faults ranges from 0.2 to 1.0 cm with steep obliquity (Fig. 4c–f).

Synsedimentary folds are mainly developed in fine-grained sediments of siltstone or mudstone with disharmony and irregularity in the liquefied sediments. The liquefaction-induced deformation of

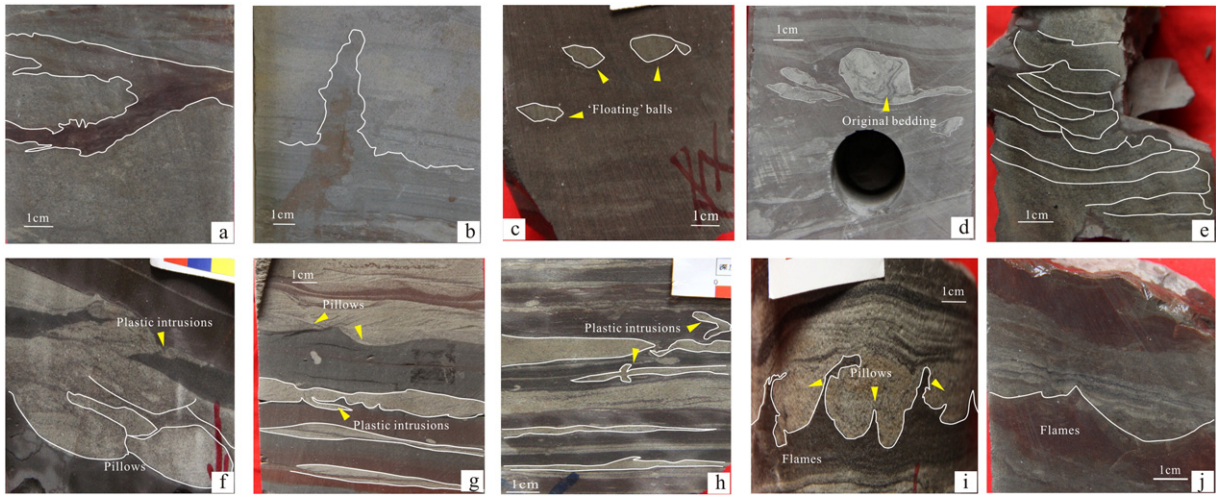


**Fig. 3.** (a–b) Plastic intrusions. (a) Plastic intrusions made of mud sediment. From well A1, at 2632.7 m. (b) Plastic intrusions made of sand sediment. From well F8, at 2522.1 m. (c–f) Ball-and-pillow structures. (c) Isolated balls ‘floating’ in mud sediment. From well A13, at 3384.2 m. (d) Balls becoming isolated from the parent rock through dragging and stretching. From well F8, at 2522.7 m. (e) Pillows arranged laterally, elliptical in shape. From well A1, at 2940.1 m. (f) Upswept pillows arranged vertically. From well B1, at 2748.1 m. (g–h) Boudinage structures. (g) Isolated boudinages in the bottom of photograph. From well B1, at 2748.8 m. (h) Boudinage structures developing with plastic intrusions. From well B1, at 2753.1 m. (i–j) Flame structures. (i) Flame structures developing with ball-and-pillow structures. From well B1, at 2923.8 m. (j) Flame structures developing with obvious liquefaction of the overlying sandstone. From well A1, at 2630.9 m.

synsedimentary folds is gentler than other SSDS that develop in association with synsedimentary faults (Fig. 4c, d). Liquefaction might result in the obliteration of laminations through complete homogenization (Mishra et al., 2013). The layers show that the deformed shapes are similar to deformed synclines and anticlines whose edges end in synsedimentary faults.

3.2. Brittle deformation structures

3.2.1. Sand dykes

Sand dykes are composed of homogeneous liquefied sandstone injected into existing cracks. During the process of deformation, small-sized breccias might fall from the surrounding rock and float within

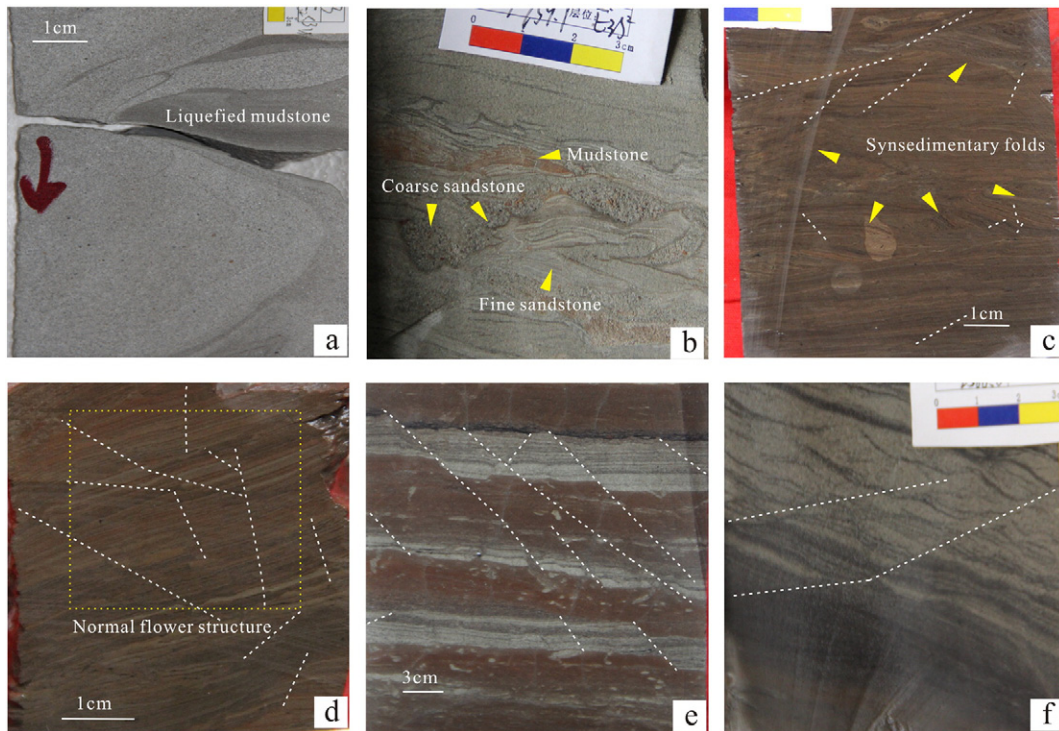


**Fig. 4.** (a) Irregular convolute stratifications observed with liquefied mudstone. From well B3, at 3005.7 m. (b) Irregular convolute stratifications mixed with fine-coarse-grained sandstone. From well B4, at 1759.7 m. (c) Synsedimentary faults developing in association with synsedimentary folds. From well A13, at 2884.7 m. (d) Synsedimentary faults developing in association with “normal flower structure”. From well A13, at 2879.5 m. (e) Synsedimentary faults developing in parallel in multiple groups. From well A1, at 2939.1 m. (f) Synsedimentary faults developing with liquefied sandstone. From well J1, at 2825.8 m.

the sand sediment. Sand dykes tend to crosscut laminated layers with steep inclination, although the morphologies of these dykes depend on the scale and nature of the cracks. The breadths of most dykes range from 0.5 to 2.0 cm and their heights are generally >10 cm. Sand dykes consist of fine-grained and well-sorted sandstone that always displays a homogenised texture (Fig. 5a, b). The injections occur after the surrounding rock, consisting of post-depositional cohesive mudstone, develops brittle fractures. The directions of the dykes could be upward or downward. The boundary between a dyke and the surrounding rock is usually clear and the two sides of the boundary present characteristics of brittle and ductile deformation, respectively. Other SSDS are frequently observed at the top of dykes (Fig. 5a, b).

### 3.2.2. Autoclastic breccias

Autoclastic breccias result from consolidated sediments, commonly represented by cohesive mudstone or fine-grained sandstone, being broken under seismic shock. The characteristics of these breccias are autochthonous, poorly sorted, angular conglomerates (Fig. 5a–d). Shattered breccias might even become spliced together (Montenat et al., 2007), and angular breccias, like spare ribs, might be distributed along the layer. In wells A13 and A1, numerous autoclastic breccias have been identified whose original sediments were silty mud (Fig. 5c–f). When fractures are sufficiently wide, they can become filled with liquefied sandstone to become plastic dykes. Liquefied sandy sediments are homogeneous with some mini breccias “floating” within them (Fig. 5e). The lengths of these poorly sorted breccias range from 1 to 5 cm and they develop with other deformation structures, e.g., ball-and-pillow and water-escape structures (Fig. 5f).

## 4. Discussion

### 4.1. Analysis on sedimentary environment of SSDS

The deposits in which SSDS are found in the study area were formed in the environments of a delta-front, shallow lacustrine facies, or at the

slope toe near the prodelta; SSDS induced by earthquakes are not found in fluvial, sub-lacustrine or other deposits. SSDS are not observed in the sediments of the delta plain because of late-stage erosion. The absence of SSDS in sub-lacustrine deposits is because of the homogeneity of the thick layer of mudstone. If sediment has no density variation, then even if a strong earthquake were to occur, deformation structures would not develop.

The SSDS developed in the thin sand–mud interbedded delta front or prodelta to lacustrine sediments are dependent on density variations. Plastic intrusions are observed more frequently in the fine-grained sediments and distributed across almost the entire delta front. Syn-sedimentary faults and folds occur mainly in underwater distributary channels and natural levees with charcoal, bioturbation, parallel bedding, and ripple bedding. Ball-and-pillow and flame structures usually develop together and they are present mainly in the delta front or near-delta lacustrine facies. Boudinage structures and irregular convolute stratifications are commonly observed in mouth bar, sheet sand of the delta front, or shallow lacustrine facies. Their grain sizes could be coarser than ball-and-pillow and flame structures. Autoclastic breccias and sand dykes are mainly observed in deposits of the slope toe near the prodelta. Their formation is based on the massive thick and cohesive mudstone that could present brittle deformation in response to a trigger mechanism. Lacustrine mudstone can be observed near the autoclastic breccias and sand dykes, containing numerous phytoclasts and testa.

### 4.2. Analysis of mechanism of SSDS formation

The characteristics of the development and distribution of SSDS in the study area accord with the criteria for their identification as seismites (Montenat et al., 2007; Owen et al., 2011). Such deformation structures have been used as indicators of seismotectonic activity in other areas or countries based on analyses of stratum sedimentary parameters (Becker et al., 2002, 2005; Nomade et al., 2005).

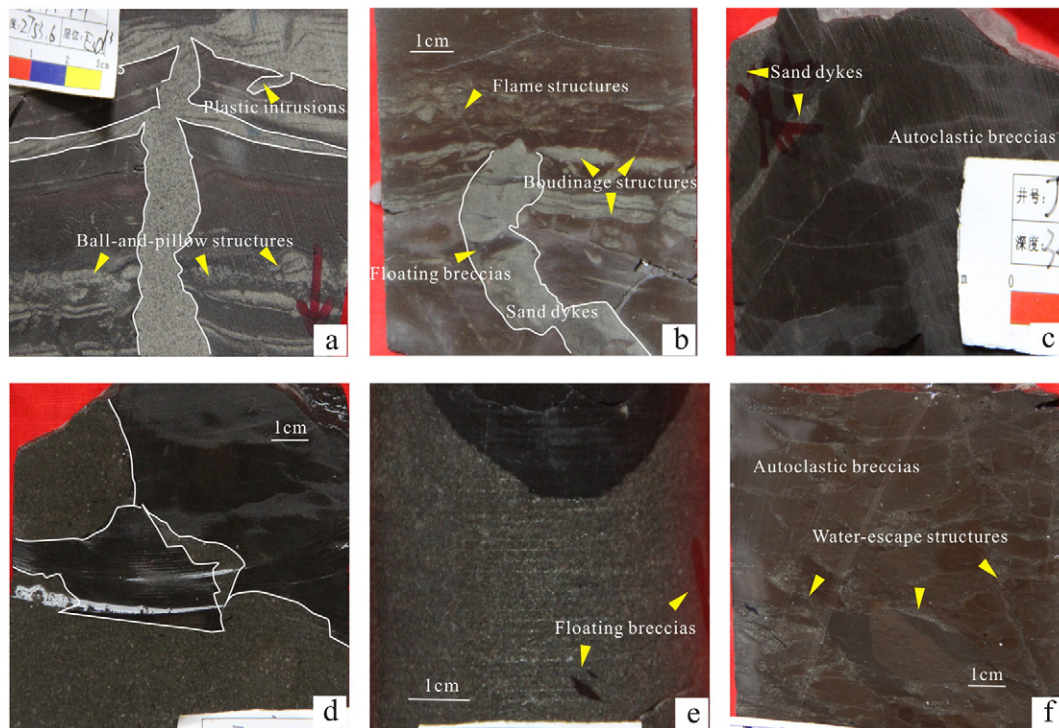


**Fig. 5.** (a–b) Sand dykes. (a) Sand dykes developing with other SSDS. From well B1, at 2753.6 m. (b) Sand dykes with other SSDS, e.g., ‘floating’ breccias within sand sediment. From well A1, at 2939.5 m. (c) Angular breccias, like spare ribs. (d) Autoclastic breccias. (e) Mini breccias ‘floating’ within homogeneous liquefied sandstone. From well A13, at 3385.8 m. (f) Autoclastic breccias developing with water-escape structures. From well A1, at 2942.5 m.

Both deformed and undeformed layers have similar lithologies and facies, indicating that the SSDS are formed in autochthonous deposits. Deposits influenced by earthquakes could be consolidated, semi-consolidated, or unconsolidated layers. Various degrees of consolidation can lead to different deformation structures under the influence of earthquake waves (Allen, 1982; Owen, 1987; Berra and Felletti, 2011). SSDS of unconsolidated layers are synsedimentary faults and folds; those of semi-consolidated strata are plastic intrusions, ball-and-pillow structures, flame structures, boudinage structures, and irregular convolute stratifications, and those of consolidated layers are sand dykes and autoclastic breccias. Unconsolidated and semi-consolidated seismites present features of ductile deformation, whereas consolidated seismites present brittle deformation structures. This means that the sediment state must have had an effect on the nature of the deformation induced by palaeo-earthquakes.

Considerable attention has been given to the relationship between the characteristics of seismites and earthquake magnitude (Scott and Price, 1988; Marco and Agnon, 1995; Mishra et al., 2013). The morphologies of SSDS are controlled by numerous factors, such as the magnitude of an earthquake, distance to the epicentre, and thickness of the sediments. The Bohai Bay basin is a long and narrow rift basin, where earthquakes are triggered mainly by tectonic activities. In the study area, the distance to the epicentre of an earthquake is essentially the same among the wells in the same oilfield. Furthermore, the thicknesses of the sediments containing the deformation structures have proven unrelated to the morphologies of the SSDS (Alfaro et al., 2010; Van Loon and Pisarska-Jamroz, 2014). Therefore, it can be safely concluded that the morphologies of SSDS in the study area, which are manifested as ductile and brittle deformation structures, depend mainly on the magnitude of the earthquake and on the degree of consolidation of the sediments. Based on previous research (Ambraseys, 1988; Marco and Agnon, 1995; Rodríguez-Pascua et al., 2000; Berra and Felletti, 2011; Van Loon and Pisarska-Jamroz, 2014), we propose that seismic activities stimulate sediments as follows. Under the effect of an earthquake of a certain magnitude (i.e.,  $M > 5$ ), sediments saturated with water will lose shear strength, leading to the process of liquefaction. When the magnitude of an earthquake is extremely large (i.e.,  $M > 8$ ), consolidated sediments will undergo brittle deformation with cracking and fracturing. During the process of seismic attenuation, less-consolidated sediments will present ductile deformation due to the liquefaction. The liquefied sediments will invade existing cracks forming sand dykes, which simultaneously have the characteristics of brittle and ductile deformation. By considering the above influencing factors, it is possible to approximate the magnitude of palaeo-earthquakes.

Plastic intrusions are typical penecontemporaneous injections of sediment, liquefied by seismic shock, which reflect the process of water escape with low fluidization velocity (Owen and Moretti, 2011). For semi-consolidated and water-saturated sediments, an earthquake of magnitude  $M = 5-6$  is sufficiently large to cause loss of shear strength and subsequent liquefaction (Lowe, 1975; Rodríguez-Pascua et al., 2010).

Synsedimentary faults and folds occur mainly in unconsolidated and fine-grained sediments that have not been separated from the original sedimentary environment. Synsedimentary faults are caused by residual stress in the post-liquefaction stage. After the phenomenon of liquefaction induced by an earthquake has ceased, the overlying sediments will undergo non-uniform settlement. The underlying sediments become re-established because of differential compaction (Owen, 1996). Synsedimentary folds and faults mainly develop together, representing slight liquefaction deformation, which requires only a relatively weak earthquake (e.g.,  $M = 3-5$ ) (Berra and Felletti, 2011).

Ball-and-pillow, flame, and boudinage structures are all load structures that occur mainly in semi-consolidated interbedded sand–mud layers of varying densities. Load structures develop persistently in lateral and continuous undulations at the interface of two types of sediment. Ball-and-pillow and flame structures develop together. Moretti and

Sabato (2007) considered that flame structures with breadths  $< 0.01$  m might have been induced by gravity, whereas larger flame structures could have been triggered by earthquakes. When denser liquefied sandy sediments fall into less-dense mud sediments, under the effects of seismic shock, the corresponding underlying and overlying layers form ball-and-pillow and flame structures (Montenat et al., 1987; Guiraud and Plaziat, 1993). A few deformed balls could present dragging and stretching morphologies. The reason for this is that liquefied sediments produce a shear force without constant direction, which leads to the balls becoming isolated from the parent rock through dragging and stretching. Boudinage structures represent ductile deformation in sediments under seismic shock. Liquefied sediments in thin layers deform under tensile stress, becoming thinner or even being pulled apart (Calvo et al., 1998; Martín-Chivelet et al., 2011). These semi-consolidated sediments deform more acutely than plastic intrusions, and they are indicative of a strong earthquake of magnitude  $M = 6-8$  (Guiraud and Plaziat, 1993; Berra and Felletti, 2011).

Irregular convolute stratifications might develop by rapid accumulation of sediments or via induced seismic shock. The formation process and morphologies of irregular convolute stratifications are similar to load structures, but without a simple interface between the layers (Owen et al., 2011). These convoluted deformation structures are supposed to have contact with seismic unconformities and when liquefied, the sediments are considered more plastic and mobile than load structures. These structures are related to hydroplastic deformation resulting from the production of excess pore pressure under seismic shock, which reduces inter-particle friction. The magnitude of an earthquake required to trigger such deformation is  $M = 6-8$  (Pöldsaaar and Ainsaar, 2015).

Autoclastic breccias occur in consolidated and cohesive sediments that undergo brittle deformation under the effects of strong seismic shock. Consolidated sediments under tremendous sheer pressure might occur as brittle deformation in shattered and autochthonous form. When fractures are well developed, crosscutting original cohesive sediments, previously fine-grained sediments become autoclastic breccias. Autoclastic breccias, which are brittle deformation structures, and sand dykes, which are ductile deformation structures, commonly develop within the same layer. The process of forming sand dykes is a consequence of brittle and ductile deformation under seismic shock. Numerous seismic-related fractures that cut across the original consolidated mudstone are developed after the climax of an earthquake. These seismic-related fractures are mainly tension fractures that can be developed in underground or surface sediments. These breccias are poorly sorted and angular, which means they are not allochthonous deposits. Breccias should be autochthonous deposits of mudstone origin, which are formed under tremendous seismic shock. The magnitude of an earthquake required to cause brittle deformation structures is greater than that necessary to form ductile deformation structures (i.e., as high as  $M = 8$ ) (Berra and Felletti, 2011; Rodríguez-Pascua et al., 2000). Consolidated mud sediments present brittle deformation, whereas sandy sediments present ductile deformation under the influence of a violent earthquake.

Based on the extent, size, and complexity of the deformation, and by considering the consolidation degree of the original sediments, we can deduce the magnitudes of palaeo-earthquakes. The SSDS induced by earthquakes can be divided into three: Group 1, Group 2, and Group 3 (Fig. 6). Group 1 comprises unconsolidated deformation structures, which are contemporaneous seismic event deposits, indicative of moderate earthquakes ( $M = 3-5$ ) with weak liquefaction. Group 2 is composed of semi-consolidated deformation structures, which are penecontemporaneous seismic event deposits, indicating moderate–strong earthquakes ( $M = 6-8$ ) with intense liquefaction. Group 3 comprises consolidated deformation structures, which are epigenetic seismic event deposits, indicative of strong earthquakes ( $M > 8$ ) with rock breaking into breccia. However, a specific seismic event could result in the occurrence of different Groups of SSDS because of differing consolidation degrees. Combinations of various SSDS can occur, mainly

	Consolidation degree	Soft-sediment deformation structures	Richter magnitude	Sedimentary structure	Groups of Seismic SSDS	Seismic intensity
Ductile deformation	Unconsolidated	Synsedimentary folds and faults	3-5		Group 1	
		Plastic intrusions	5-6			
	Semi-consolidated	Ball-and-pillow structures	6-8		Group 2	
		Flame structures	6-8			
		Boudinage structures	6-8			
		Irregular convolute stratifications	6-8			
Brittle deformation	Consolidated	Sand dykes	7-8		Group 3	
		Autoclastic breccias	>8			

Fig. 6. Groups of SSDS and possible range of magnitude of the palaeoearthquake (modified from Berra and Felletti, 2011).

comprising those of Group 2 or of Groups 1 and 2. These Groups, depending on the combination of SSDS, might not appear at the same time. Thus, when the magnitude of an earthquake is sufficiently large, it is possible that its effects will be recorded in the strata. We can trace seismic events in terms of spatial stratigraphic aspects and determine basin tectonic activities based on the SSDS information.

A model of seismically induced SSDS can be established in combination with the sedimentary environment and deformation groups, reflecting the production and preservation of SSDS in this basin. (See Fig. 7.) It is concluded that SSDS occur across facies under a seismic event. The SSDS of group 3 mainly distribute at the slope toe or the

prodelta, whereas the SSDS of groups 2 and 1 mainly distribute in the distal and proximal bars of the delta front, respectively. During the process of an intense seismic event, consolidated sediments initially form SSDS of group 3. Then, less-consolidated sediments form SSDS of groups 1 and 2 in response to seismic attenuation. The extents of the deformation structures decrease successively from the prodelta to the proximal bar of the delta front. Therefore, judgement of seismic intensity is dependent on the biggest group of SSDS. Seismites distribute on slopes, regardless of the grade. These slopes not only create instability in the liquefied sediments, meaning they could be sediments susceptible to the formation of SSDS (Allen, 1982), but they also provide sufficient

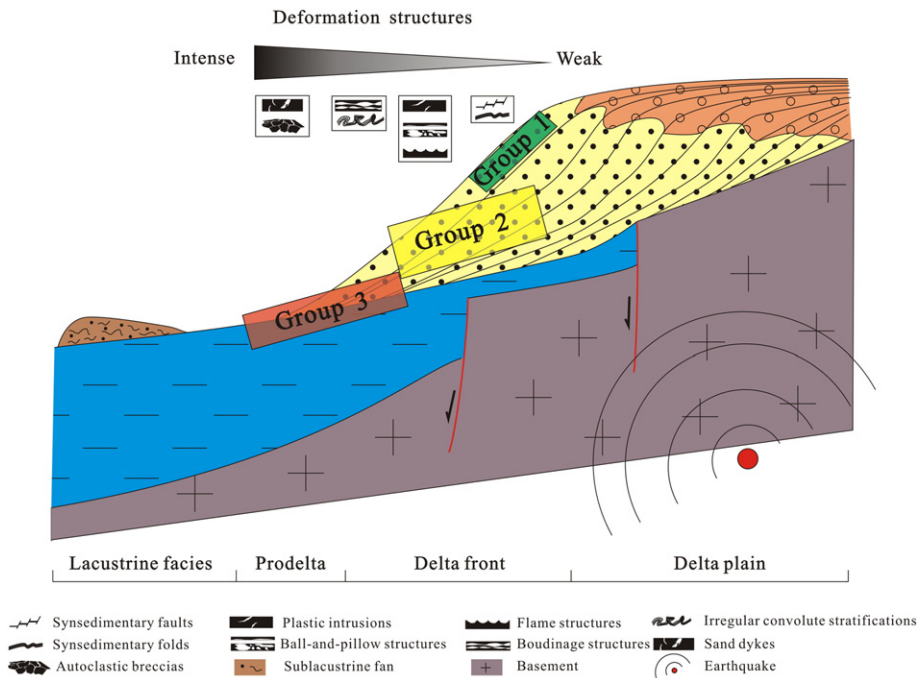


Fig. 7. Development model of SSDS in the Palaeogene deposits of the Liaodong Bay Depression.

accommodation within which to preserve SSDS. The deposits of a sub-lacustrine fan could be interpreted as due to a seismic trigger; however, the sediments in a sub-lacustrine fan are gravity-driven and allochthonous with coarse gravel reflecting slumps, turbidites, or sandy debris flows.

#### 4.3. Spatial distribution of SSDS

In the study area, the core wells are mainly distributed in the Liaodong Uplift, Liaoxi Uplift, and Liaozhong Sag. Among these wells, those in which SSDS are observed are distributed in the NE direction along the Tan–Lu faults. The wells with developed SSDS converge on the A and B oilfields or nearby areas (Fig. 8a, b). The strike-slip tectonic activity of the Tan–Lu faults, being a continuous phenomenon, has led to the release of stress along the fault system and to the recurrence of SSDS. Apparently, the distribution of SSDS is controlled by the Tan–Lu faults, which remain the controlling faults of the basin. The concentration of seismic events indicates intense tectonic activity in these areas. Hence, it is believed that the A and B oilfields represent the Palaeogene centres of tectonic activity of the west and east branches of the Tan–Lu faults, respectively.

The A oilfield is at the northern head of the Liaoxi Uplift. Palaeo-earthquake activities in the A oilfield were primarily moderate or occasionally strong (Fig. 8a, b). The fall of the basement of the A oilfield was considerable, causing intense tectonic activity. The A oilfield and Liaoxi Uplift were formed because of extensional activities of the west branch faults, which explains the absence of SSDS at the southern head of the Liaoxi Uplift. In the A oilfield, the well cores indicate the development of migration of seismites in the east direction from  $E_2s^3$  because of the dextral slip activity. Fewer SSDS in the A oilfield are observed in the Dongying Fm. indicating the tectonic activity of the west branch faults declined significantly during the period of its formation (Fig. 8a, b).

The B oilfield is in the middle of the east branch faults, which pass through the Liaozhong Sag. Seismic activities in the B oilfield are more concentrated than in the A oilfield. Palaeo-earthquake activities in the B oilfield were dominated by moderate–strong and moderate earthquakes throughout the entire Palaeogene (Fig. 8a, b). This indicates the east branch faults were active from the time of the Shahejie Fm. to the Dongying Fm. The east branch faults are steep dip faults dominated by strike-slip activity. The B oilfield lies just within the tectonic reverse area, formed by the enhancement of strike-slip activity, which has resulted in the mud diapir and stratigraphic inversion. The tectonic

inverted structures controlled by the east branch faults extend along the Liaozhong Sag in the NE direction, and the B oilfield is at the point of the most drastic tectonic inversion. This explains why so many SSDS converge in the B oilfield and why they are indicative of relatively stronger magnitudes.

#### 4.4. Stratigraphic distribution of SSDS

Because the SSDS are concentrated mainly in the A and B oilfields, their stratigraphic distribution is studied to determine the tectonic activities of the A and B oilfields. SSDS can be traced laterally within the same sequence and therefore, we can expect to establish the evolution of the regulation by the Tan–Lu faults via connected well sections (Zheng et al., 2015). SSDS are observed from  $E_2s^3$  to  $E_3d^1$ , which means that seismic events occurred throughout the entire Palaeogene, even during the extinct rifting stage ( $E_2s^2$ – $E_2s^1$ ). There are hardly any SSDS observed in  $E_3d^{2u}$  and  $E_3d^1$ . The main reason for this is that their strata thicknesses are thin or eroded because of the integral uplift of the basin. The occurrence of SSDS in the vertical is discontinuous but repetitive, suggesting that the occurrence of palaeo-earthquakes was episodic, i.e., similar to modern earthquakes.

The coring intervals and cores with SSDS are shown in Fig. 9a, with the Groups of SSDS classified. In the A oilfield, SSDS are mainly observed in the Shahejie Fm. SSDS of Group 3 are observed in well A13 in  $E_2s^3$ , which indicates that the magnitudes of palaeo-earthquakes in the A oilfield were very strong (i.e.,  $M > 8$ ). SSDS of Group 2 are observed in almost all areas (wells A1, A4, A13, A5, A3 and C5) in  $E_2s^2$ , which have continuous lateral development, suggesting that the palaeo-earthquakes reflected by  $E_3s^2$  were relatively stronger. In  $E_2s^1$ , only Group 1 SSDS are observed in well A13, so minimal seismic activity in  $E_2s^1$  can be inferred. In wells A1 and C5, SSDS of Groups 3 and 2 are developed in  $E_3d^2$ , indicating the magnitudes of palaeo-earthquakes increase again in  $E_3d^2$ . In comparison, fewer SSDS exist in  $E_3d^3$ , but this might be due to the distribution of the core intervals. Based on the spatial stratigraphic distribution of SSDS and the magnitudes of palaeo-earthquakes, we can infer that the extensional tectonic activities of the A oilfield in the west branch faults decreased sharply from  $E_2s^3$  to  $E_2s^1$  and increased again in  $E_3d^2$  (Fig. 9b).

The B oilfield lies within the east branch faults in the middle of Liaozhong Sag. Above the seismites, numerous sub-lacustrine fan deposits indicate that gravity flows in this area might have been induced by earthquakes (Fig. 10a). SSDS developed in the B oilfield can be traced

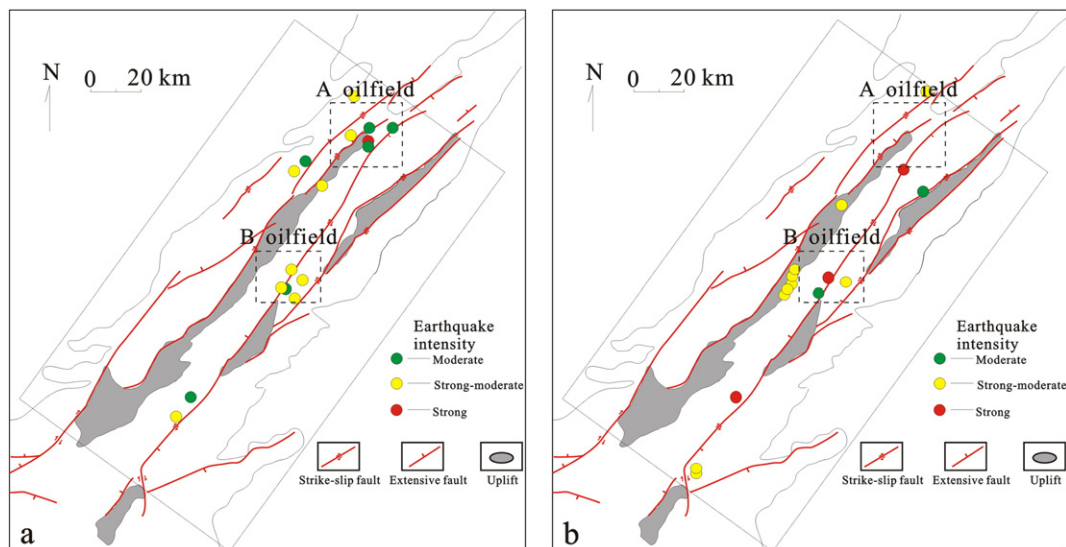
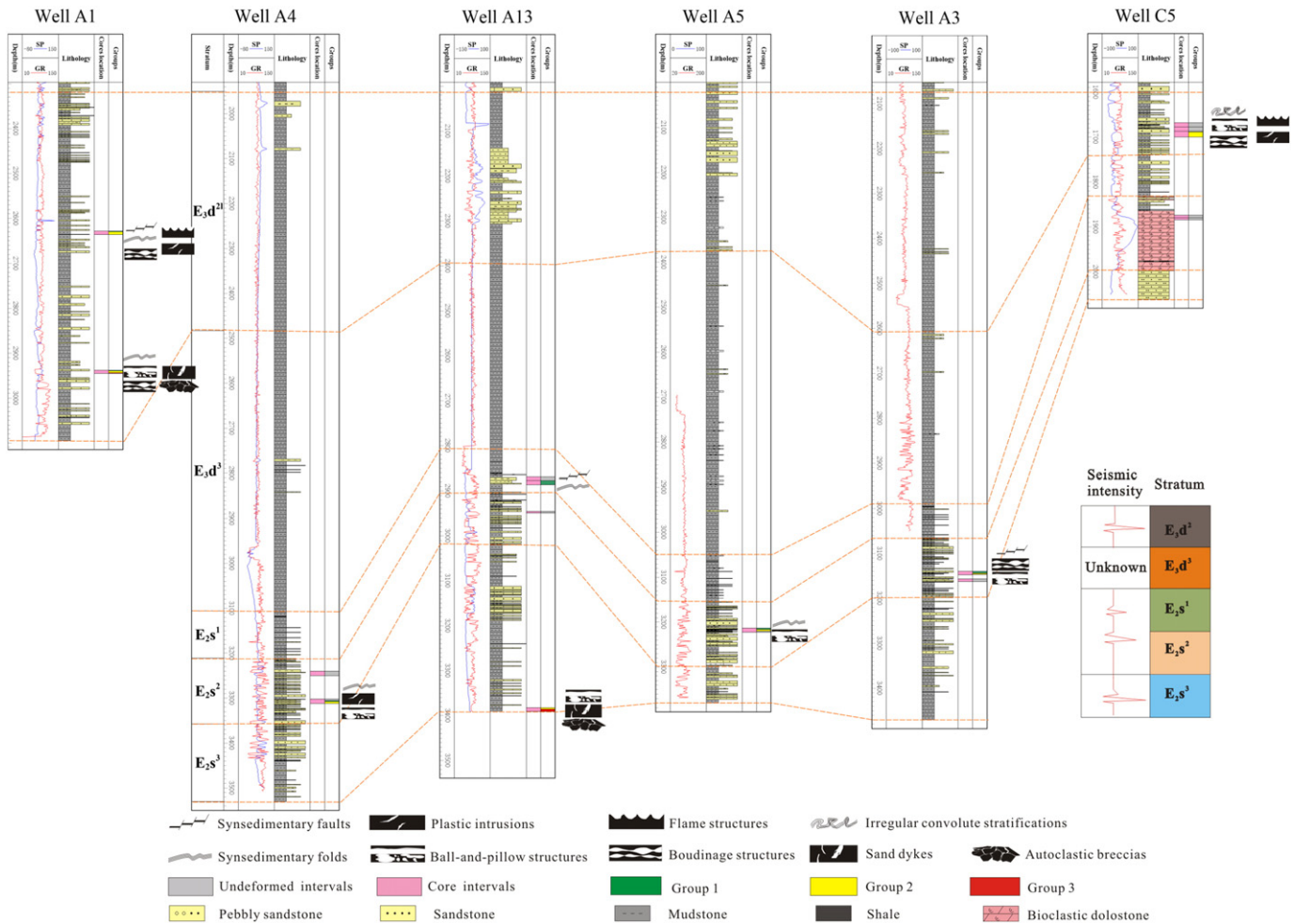


Fig. 8. (a) Spatial distribution of earthquakes in the Shahejie Formation. (b) Spatial distribution of earthquakes in the Dongying Formation.



**Fig. 9.** (a) Stratigraphic distribution of SSDS in the cores from the A oilfield. See Fig. 1b for the location of section A–A'. (b) Proposed seismic intensity from  $E_{2s^3}$  to  $E_{3d^2}$  of the west branch faults in the Liaodong Bay Depression. Note: the seismic intensity is relative, not exact.

laterally, as in the A oilfield. In  $E_{2s^3}$  and  $E_{2s^2}$ , in contrast with the A oilfield, SSDS in the B oilfield are dominated by those of Groups 1 and 2 (wells B1, B1 and B3), but especially Group 1. The SSDS tend toward those of Group 2 in  $E_{2s^1}$ , which indicates a strengthening of the palaeo-earthquakes reflected in  $E_{2s^1}$ . From  $E_{2s^3}$  to  $E_{2s^1}$ , the palaeo-earthquake intensity shows a gradual increasing trend, according to the variation of the morphologies of the SSDS. Moreover, the palaeo-earthquake intensities reached their maximum in  $E_{3d^3}$ , as indicated by SSDS of Groups 3 and 2 (wells B2 and B1), before gradually diminishing in  $E_{3d^2}$ . The palaeo-earthquake intensity reflects the strike–slip tectonic activities of the east branch faults in the B oilfield, which should correspond to the variation law of palaeo-earthquakes (Fig. 10b).

## 5. Conclusions

- (1) An approximately 200-m-long section of SSDS was observed in 21 wells in the Palaeogene deposits of the Liaodong Bay Depression, which contained plastic intrusions, ball-and-pillow structures, flame structures, boudinage structures, synsedimentary faults and folds, irregular convolute stratifications, sand dykes, and autoclastic breccias. Based on their deformation features, the SSDS were divided into two groups: ductile and brittle deformation structures.
- (2) Based on an analysis of the sedimentary environment, the observed SSDS in the Liaodong Bay Depression were found mainly developed in delta front and shallow lacustrine facies. Ductile

deformation structures, observed in interbedded sand and mud layers, reflected deformation of unconsolidated and semi-consolidated sediments. In contrast, brittle deformation structures were found in mudstone or fine-grained sediments, reflecting deformation of consolidated deposits.

- (3) These SSDS were induced by palaeo-earthquakes and their morphologies reflect the earthquake intensity. The magnitude required of an earthquake to cause liquefaction is approximately  $M = 5$ . When the magnitude increases to  $M = 8$ , brittle deformation might result. Based on information regarding ductile and brittle deformation, the SSDS were divided into three Groups that reflected palaeo-earthquake intensity. The SSDS, classified by morphology, reflected the decreasing magnitude of palaeo-earthquakes in the following order: Group 3 > Group 2 > Group 1. With consideration of the palaeo-sedimentary environment, we proposed a model to account for the production and preservation of the SSDS. The extents of the deformation structures decrease successively from the prodelta to the proximal bar of the delta front.
- (4) The spatial and stratigraphic distributions of SSDS in the well cores were used to infer the tectonic activities of the Tan–Lu faults, in combination with the morphologies of the SSDS. The Tan–Lu faults comprise two branches of faults, the tectonic activities of which have been focused on the A and B oilfields, respectively. The extensional tectonic activities of the west branch faults in the A oilfield exhibit a sharply decreasing trend from  $E_{2s^3}$  to  $E_{2s^1}$ , and increase

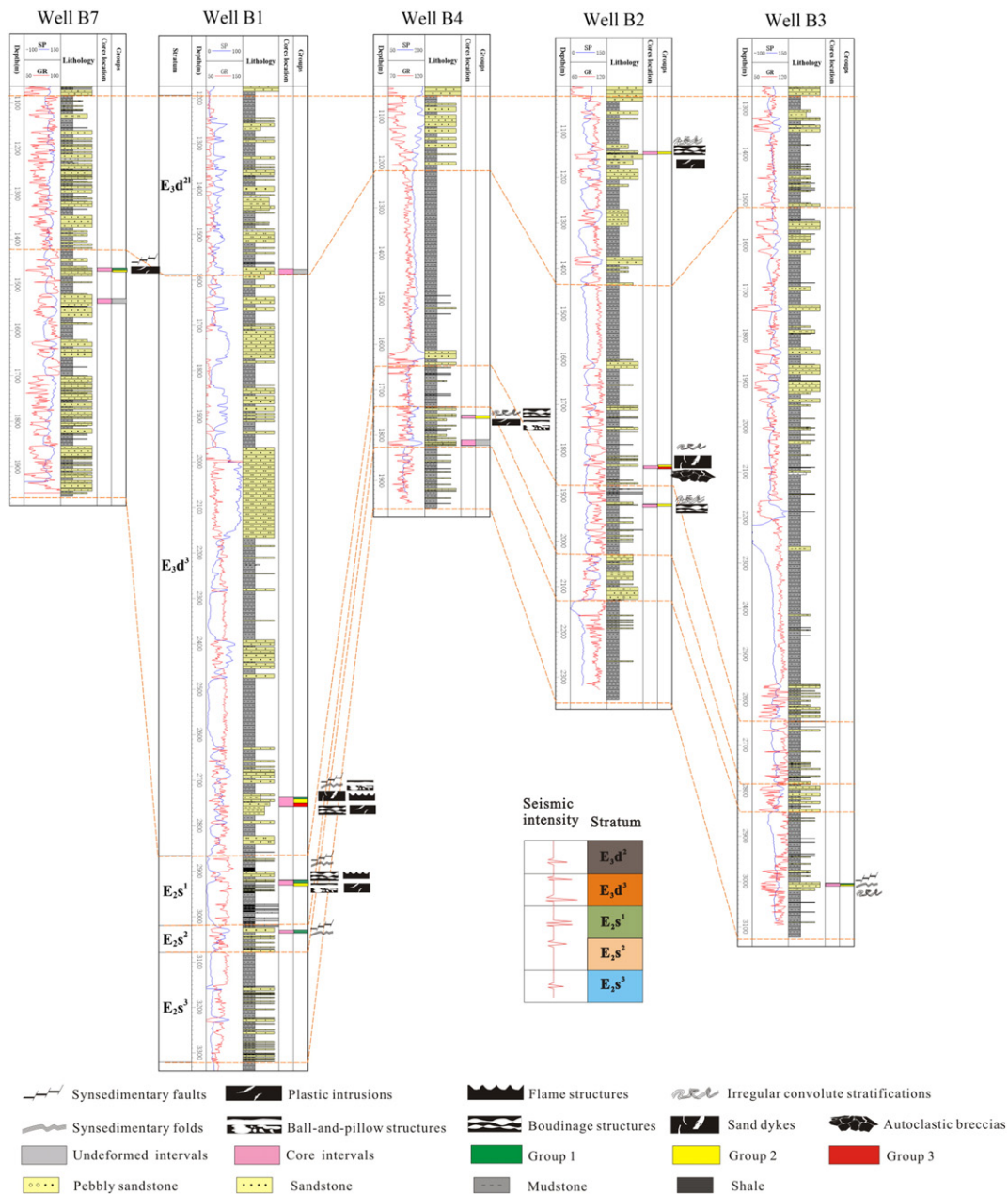


**Fig. 10.** (a) Stratigraphic distribution of SSDS in the cores from the B oilfield. See Fig. 1b for the location of section B–B'. (b) Proposed seismic intensity from  $E_2s^3$  to  $E_3d^2$  of the east branch faults in the Liaodong Bay Depression. Note: the seismic intensity is relative, not exact.

again in  $E_3d^2$ . However, intensity of the strike-slip tectonic activities in the east branch faults shows an increasing trend from  $E_2s^3$  to  $E_2s^1$ , with the intensity reaching a climax in  $E_3d^3$ .

- (5) This study attempted to establish the tectonic activity of the Tan-Lu faults based on spatial and stratigraphic aspects according to palaeo-earthquake activity. It was demonstrated that the results derived from the distribution of SSDS were consistent with previous studies. Analysis of the SSDS distribution can provide supplemental information that can help explain the dynamic evolution of both basin-controlling faults and basin tectonics.

**References**

Alfaro, P., Delgado, J., Estévez, A., Molina, J.M., Moretti, M., Soria, J.M., 2002. Liquefaction and fluidization structures in Messinian storm deposits (Bajo Segura Basin, Betic Cordillera, southern Spain). *International Journal of Earth Sciences* 91, 505–513.

Alfaro, P., Gibert, L., Moretti, M., García-Tortosa, F.J., Sanz de Galdeano, C., Galindo-Zaldívar, J., López-Garrido, T.C., 2010. The significance of giant seismites in the Plio-Pleistocene Baza palaeo-lake (S Spain). *Terra Nova* 22, 172–179.

Allen, J.R.L., 1982. *Sedimentary Structures: Their Character and Physical Basis*. Vol. II. Elsevier, New York (663 pp.).

Ambraseys, N.N., 1988. Engineering seismology. *Earthquake Engineering and Structural Dynamics* 17, 1–105.

Bachmann, G.H., Aref, M.A.M., 2005. A seismite in Triassic gypsum deposits (Grabfeld Formation, Ladinian), southwestern Germany. *Sedimentary Geology* 180, 75–89.

Becker, A., Davenport, C.A., Giardini, D., 2002. Palaeoseismicity studies on end-Pleistocene and Holocene lake deposits around Basle, Switzerland. *Geophysical Journal International* 149, 659–678.

Becker, A., Davenport, C.A., Rodríguez-Pascua, M.A., 2005. Detailed drill core analysis for the reconstruction of palaeoenvironmental events and prehistoric earthquakes from sediment structures in Lake Seewen, Switzerland. *Zeitschrift für Geologische Wissenschaften* 33, 401–431.

Berra, F., Felletti, F., 2011. Syn depositional tectonics recorded by soft-sediment deformation and liquefaction structures (continental Lower Permian sediments, Southern Alps, Northern Italy): stratigraphic significance. *Sedimentary Geology* 235, 249–263.

- Calvo, J.P., Rodríguez-Pascua, M.A., Martín-Velázquez, S., Jiménez, S., De Vicente, G., 1998. Microdeformation of lacustrine laminite sequences from Late Miocene formations of SE Spain: an interpretation of loop bedding. *Sedimentology* 45, 279–292.
- Chaney, R.C., Fang, H.Y., 1991. Liquefaction in the coastal environment: an analysis and case histories. *Marine Geotechnology* 10, 343–370.
- Chang, Y.Y., Lin, C.S., Zhou, X.H., Xia, S.Q., 2014. Depositional sequences and prediction of favorable reservoir sand of Shahejie Formation of Liaoxi Depression. *Earth Science Journal of China University of Geosciences* 39, 1471–1480.
- Chen, S.Y., Yuan, W.F., Yan, J.H., 2003. Discovery and significance of earthquake event deposits of Early Tertiary in the Jiyang Depression. *Chinese Journal of Geology* 38, 377–384 (in Chinese with English abstract).
- Dong, Y.L., Zhu, X.M., Li, D.J., Yang, J.S., Zhang, Y.Y., Zhu, S.F., 2007. Seismic facies of Paleogene in Liaodong Bay, Bohai basin. *Acta Sedimentologica Sinica* 25, 554–563.
- Galli, P., 2000. New empirical relationships between magnitude and distance for liquefaction. *Tectonophysics* 324, 169–187.
- Ghosh, S.K., Singh, S.S., Ray, Y., Sinha, S., 2010. Soft-sedimentary deformational structures: seismites or penecontemporaneous, a study from the Palaeoproterozoic Lesser Himalayan succession, India. *Current Science* 98, 247–253.
- Gong, Z.S., Cai, D.S., Zhang, G.C., 2007. Dominating action of Tanlu Fault on hydrocarbon accumulation in eastern Bohai Sea area. *Acta Petroleologica Sinica* 28, 1–9 (in Chinese with English abstract).
- Guiraud, M., Plaziat, J.C., 1993. Seismites in the fluvialite Bima sandstones: identification of palaeoseisms and discussion of their magnitudes in a Cretaceous synsedimentary strike-slip basin (Upper Benue, Nigeria). *Tectonophysics* 225, 493–522.
- Jewell, H.E., Ertensohn, F.R., 2004. An ancient seismite response to Taconian far-field forces: the Cane Run Bed, Upper Ordovician (Trenton) Lexington Limestone, central Kentucky (USA). *Journal of Geodynamics* 37, 487–511.
- Kundu, K., Matin, A., Mukul, M., Eriksson, P.G., 2011. Sedimentary facies and soft-sediment deformation structures in the Late Miocene Pliocene Middle Siwalik subgroup, Eastern Himalaya, Darjiling District, India. *Journal of the Geological Society of India* 78, 321–326.
- Li, D.J., Zhu, X.M., Dong, Y.L., Zhang, X.J., Chen, J.Q., Sun, Q., Xiong, Z.W., 2007. Sequence stratigraphy and depositional system of Paleogene Shahejie Formation in Liaodong Bay Depression. *Petroleum Exploration and Development* 34, 669–767.
- Lowe, D.R., 1975. Water-escape structures in coarse-grained sediments. *Sedimentology* 22, 157–204.
- Lu, S.Q., 2004. Study on the distinguishing marks of seismites in clastic rock strata of Palaeogene in Jiyang Depression. *Journal of China University of Petroleum* 30, 8–13 (in Chinese with English abstract).
- Marco, S., Agnon, A., 1995. Prehistoric earthquake deformations near Masada, Dead Sea Graben. *Geology* 23, 695–698.
- Martín-Chivelet, J., Palma, R.M., López-Gómez, J., Kietzmann, D.A., 2011. Earthquake induced soft-sediment deformation structures in Upper Jurassic open-marine microbialites (Neuquén Basin, Argentina). *Sedimentary Geology* 235, 210–221.
- Mishra, A., Srivastava, D.C., Shah, J., 2013. Late Miocene–Early Pliocene reactivation of the Main Boundary Thrust: evidence from the seismites in southeastern Kumaun Himalaya, India. *Sedimentary Geology* 289, 148–158.
- Montenat, C., Barrier, P., d'Estevou, P.O., Hibsich, C., 2007. Seismites: an attempt at critical analysis and classification. *Sedimentary Geology* 196, 5–30.
- Montenat, C., Ott D'Estevou, P., Masse, P., 1987. Tectonic–sedimentary characters of the Betic Neogene basins evolving in a crustal transcurrent shear zone (SE Spain). *Bulletin des Centres de Recherches Exploration-Production Elf-Aquitaine* 11, 1–22.
- Moretti, M., Ronchi, A., 2011. Liquefaction features interpreted as seismites in the Pleistocene fluvio-lacustrine deposits of the Neuquen Basin (Northern Patagonia). *Sedimentary Geology* 235, 200–209.
- Moretti, M., Sabato, L., 2007. Recognition of trigger mechanisms for soft-sediment deformation in the Pleistocene lacustrine deposits of the Sant'Arcangelo Basin (southern Italy): seismic shock vs. overloading. *Sedimentary Geology* 196, 31–45.
- Nomade, J., Chapron, E., Desmet, M., Reyss, J.L., Arnaud, F., Lignier, V., 2005. Reconstructing historical seismicity from lake sediments (Lake Laffrey, Western Alps, France). *Terra Nova* 17 (4), 350–357.
- Obermeier, S.F., 1996. Use of liquefaction-induced features for palaeoseismic analysis. An overview of how seismic liquefaction features can be distinguished from other features and how their regional distribution and properties of source sediment can be used to infer the location and strength of Holocene palaeo-earthquakes. *Engineering Geology* 44, 1–76.
- Oliveira, C.M.M., Hodgson, D.M., Flint, S., 2011. Distribution of soft-sediment deformation structures in clinoform successions of the Permian Ecca Group, Karoo Basin, South Africa. *Sedimentary Geology* 235, 314–330.
- Owen, G., 1987. Deformation processes in unconsolidated sands. In: Jones, M.E., Preston, R.M.F. (Eds.), *Deformation of Sediments and Sedimentary Rocks*. Geological Society Special Publication Vol. 29, pp. 11–24.
- Owen, G., 1996. Experimental soft-sediment deformation: structures formed by the liquefaction of unconsolidated sands and some ancient examples. *Sedimentology* 43, 279–293.
- Owen, G., Moretti, M., 2011. Identifying triggers for liquefaction-induced soft-sediment deformation in sands. *Sedimentary Geology* 235, 141–147.
- Owen, G., Moretti, M., Alfaro, P., 2011. Recognising triggers for soft-sediment deformation: current understanding and future directions. *Sedimentary Geology* 235, 133–140.
- Pöldsaa, K., Ainsa, L., 2015. Soft-sediment deformation structures in the Cambrian (Series 2) tidal deposits (NW Estonia): implications for identifying endogenic triggering mechanisms in ancient sedimentary record. *Palaeoworld* 24, 16–35.
- Rodríguez-Pascua, M.A., Calvo, J.P., De Vicente, G., Gómez-Gras, D., 2000. Soft-sediment deformation structures interpreted as seismites in lacustrine sediments of the Prebetic Zone, SE Spain, and their potential use as indicators of earthquake magnitudes during the Late Miocene. *Sedimentary Geology* 135, 117–135.
- Rodríguez-Pascua, M.A., Garduño-Monroy, V.H., Israde-Alcántara, I., Pérez-López, R., 2010. Estimation of the palaeoepicentral area from the spatial gradient of deformation in lacustrine seismites (Tierras Blancas Basin, Mexico). *Quaternary International* 219, 66–78.
- Rossetti, D.F., Góes, A.M., 2000. Deciphering the Sedimentological imprint of palaeoseismic events: an example from the Aptian Codo Formation, northern Brazil. *Sedimentary Geology* 135, 137–156.
- Scott, B., Price, S., 1988. Earthquake-induced structures in young sediments. *Tectonophysics* 147, 165–170.
- Seilacher, A., 1969. Fault-grade bed interpreted as seismite. *Sedimentology* 13, 155–159.
- Shi, Y.J., Chen, W.J., Cao, Z.L., Li, H.Z., Wang, B.T., Huang, S.J., 2009. Discovery of seismites in the Southwestern Qaidam Basin and its significance for exploration. *Acta Geologica Sinica* 83, 1178–1187 (in Chinese with English abstract).
- Sims, J.D., 1975. Determining earthquake recurrence intervals from deformational structures in young lacustrine sediments. *Tectonophysics* 29, 141–152.
- Taggin, C.K., 2011. Seismically-generated hydroplastic deformation structures in the Late Miocene lacustrine deposits of the Malatya Basin, eastern Turkey. *Sedimentary Geology* 235, 264–276.
- Van Loon, A.J., Pisarska-Jamroz, M., 2014. Sedimentological evidence of Pleistocene earthquakes in NW Poland induced by glacio-isostatic rebound. *Sedimentary Geology* 300, 1–10.
- Wang, Y.J., Wang, J., Zhou, X.H., Teng, Y.B., Chen, A.Q., 2008. Study of characteristic of Palaeogene seismoturbidite in the central Liaozhong depression, Liaodong Bay. *Journal of Mineralogy and Petrology* 28, 84–89.
- Wu, W., Lin, C.S., Zhou, X.H., Dong, W., Li, Q., Zheng, J.G., 2011. High-resolution sequence stratigraphy and depositional system analysis of Dongying Formation, Paleogene in Liaozhong Depression. *Geological Science and Technology Information* 30, 63–70.
- Xu, C.G., Xu, X.S., Qiu, D.Z., Lai, W.C., Zhou, X.H., 2005. Structural and sequence stratigraphic frameworks and palaeogeography of the Palaeogene in central-southern Liaoxi sag, Liaodongwan Bay area. *Journal of Palaeogeography* 7, 449–459 (in Chinese with English abstract).
- Yuan, J., 2004. The property and geological significance of seismites of Palaeogene in Huimin sag, Shandong province. *Acta Sedimentologica Sinica* 22, 41–46 (in Chinese with English abstract).
- Zhang, C.H., Wu, Z.J., Gao, L.Z., Wang, W., Tian, Y.L., Ma, C., 2007. Earthquake-induced soft-sediment deformation structures in the Mesoproterozoic Wumishan Formation, North China, and their geologic implications. *Science in China Series D: Earth Sciences* 50, 350–358.
- Zhao, C.L., Yang, C.X., Liu, M.H., 1996. The Lithofacies–Palaeogeography of Continental Clastic of Palaeogene, Bohai Basin. Petroleum Industry Press, Beijing.
- Zheng, L.J., Jiang, Z.X., Liu, H., Kong, X.X., Li, H.P., Jiang, X.L., 2015. Core evidence of paleoseismic events in Paleogene deposits of the Shulu Sag in the Bohai Bay Basin, east China, and their petroleum geologic significance. *Sedimentary Geology* 328, 33–54.
- Zhu, X.M., Dong, Y.L., Yang, J.S., Zhang, Q., Li, D.J., Xu, C.G., Yu, S., 2008. The sequence framework and depositional system distribution of Paleogene in Liaodong Bay area. *Science in China Series D: Earth Sciences* 38 (Suppl. 1), 1–10 (in Chinese with English abstract).